Effect of the surface polarization in polar perovskites studied from first principles

M. Fechner,[1] S. Ostanin,[1] and I. Mertig[1,2]
[1]*Max-Planck-Institut für Mikrostrukturphysik, Weinberg 2, D-06120 Halle (Saale), Germany*
[2]*Martin-Luther-Universität Halle-Wittenberg, Fachbereich Physik, D-06099 Halle, Germany*
(Received 7 December 2007; published 11 March 2008)

The (001) surfaces of polar perovskites $BaTiO_3$ and $PbTiO_3$ have been studied from first principles at $T=0$ K. For both cases of polarization, the most stable TiO-terminated interfaces show intrinsic ferroelectricity. In the topmost layer, where the O atoms are >0.1 Å above Ti, this leads to metallic instead of the insulating behavior of the electronic states that may have important implications for multiferroic tunneling junctions.

DOI: 10.1103/PhysRevB.77.094112 PACS number(s): 31.15.A−, 68.47.Gh, 73.20.At, 77.84.Dy

Epitaxial growth technique opens the way to combine ferroelectrics (FEs) and ferromagnets into multicomponent multiferroics, which are inaccessible by traditional synthesis.[1,2] Currently, many laboratories across the world work on a prototypical device, consisting of a few nanometer thick ferroelectric sandwiched between a ferromagnet and another metallic contact. External electric field applied to the FE phase causes a switching of its polarization **P** that, in turn, through the magnetoelectric coupling may change the magnetic order in the ferromagnetic phase.[3] Altering **P** and magnetization independently for encoding information in multiferroics, the smallest quaternary logical memory might be obtained. Fundamentally new multiferroics require a better understanding of the FE order parameters; especially, in the case of thin films here the symmetry is reduced.

Since direct measurements of atomic displacements, occurring in FE near the interface, are extremely challenging, their structures can be understood and numerically characterized from first principles. Recently, much work has been conducted to study bare FE surfaces using the *ab initio* density functional theory (DFT) calculations.[4–12] It has been found that the critical thickness down to 3 unit cells (1.2 nm) is enough to enable the existence of ferroelectricity at room temperature.[13–15] However, there are only some convincing evidences in the literature, i.e., the work by Cohen[5] that the direction of **P** may affect the surface relaxation. The functionality of multiferroics assumes that **P** must be reversible and parallel to the surface normal. Hence, it is worthwhile to carry out *ab initio* calculations which model the reaction of the (001) surface of polar ferroelectric surfaces upon the change of its reversible **P**.

In this paper, we study the (001) surface of ABO_3 perovskites (A=Sr, Ba, Pb and B=Ti), which represent a wide class of ferroelectrics ranging from paraelectric $SrTiO_3$ (STO) to highly polar $PbTiO_3$ (PTO), while $BaTiO_3$ (BTO), with its moderate spontaneous polarization P_s, is an example of a typical FE. The study is based on extensive calculations, using the Vienna *ab initio* simulation package[16] (VASP), in which the effects of relaxation of atomic positions are included. Nowadays, many FE properties can be successfully calculated from first principles.[17] Table I collects the experimental data for the lattice parameters and atomic positions, obtained for the room-temperature tetragonal phase of PTO and BTO (with space group symmetry $P4mm$) and for cubic STO ($Pm\text{-}3m$), in comparison with our calculation. Overall, there is a good agreement between the measured and theoretical structure parameters for the three systems. For polar BTO and PTO, their values of **P**, calculated by the Berry phase approach,[22,23] are in reasonably good agreement with the experiment. The minor differences, seen in Table I between our and some other recent DFT results,[6,12,24] can be attributed to the choice of pseudopotentials and/or to the approximation used for the exchange and correlation potentials. We used the local density approximation (LDA), while the electron-ion interactions were described by the PAW pseudopotentials. After relaxation, the calculated forces are always less than 0.5×10^{-2} eV/Å. The electron pseudo-wavefunctions were represented using plane waves, with a cutoff energy of 650 eV. For the Brillouin-zone integration, a dense Monkhorst-Pack[25] mesh was used.

We calculated a 5 unit cell (~2 nm) thick ABO_3 film. The atoms of the two upper or, alternatively, two lower unit cells were allowed to relax, while all other atoms in the supercell were fixed at their bulklike and previously optimized posi-

TABLE I. The lattice parameters a, c/a, fractional atomic coordinates, z/a, and polarization, calculated for the room-temperature PTO, BTO, and STO phases, are shown in comparison with the corresponding experimental data.

		PTO	BTO	STO
a (Å)	Expt.	3.892[a]	3.991[b]	3.898[b]
		3.858	3.943	3.885
c/a	Expt.	1.071[a]	1.011[b]	1.0
		1.071	1.013	
Ti	Expt.	0.542[a]	0.489[b]	0.5
		0.542	0.492	
O-1, 2	Expt.	0.629[a]	0.511[b]	0.5
		0.622	0.513	
O-3	Expt.	0.124[a]	0.018[b]	0.0
		0.115	0.021	
P_s (μC/cm^2)	Expt.	75[c]	26[d]	
		94.3	22.9	

[a]Reference 18.
[b]Reference 19.
[c]Reference 20.
[d]Reference 21.

TABLE II. The surface energy E_{surf} (in eV) for the TiO_2- and AO-terminated (001) surfaces and the cation-anion displacements δ (in Å) calculated for the top five layers of the perovskite (001) surfaces.

	PTO		BTO		STO
	$P_\uparrow$	$P_\downarrow$	$P_\uparrow$	$P_\downarrow$	$P=0$
E_{surf} (AO)	2.21	2.46	1.49	1.63	1.36
E_{surf} (TiO_2)	2.07	2.20	1.31	1.32	1.34
ML					
(1) O-Ti	0.108	0.233	0.102	0.129	0.072
(2) O-A	−0.316	0.260	−0.086	−0.030	0.118
(3) O-Ti	−0.153	0.201	−0.002	0.067	0.018
(4) O-A	−0.476	0.476	−0.082	0.082	0.0
(5) O-Ti	−0.333	0.333	−0.086	0.086	0.0

tions, which are shown in Table I. A vacuum spacer of 2 nm was used to separate the copies of the periodic structures in the direction perpendicular to the surface. The ABO_3 perovskite structures possess a strong anisotropy resulting in the AO (A=Pb,Ba) and TiO_2 layers alternating in the [001] direction. The (001) surface of an ABO_3 can be terminated by a AO or a TiO_2 layer. Recently, Eglitis and Vanderbilt[12] have reported for the cubic structure of BTO and PTO that the TiO_2-terminated surface is more stable. Using the same approach,[12] we calculated the surface energy for the both terminations of ABO_3. The results are shown in Table II. For each perovskite, its TiO_2-terminated (001) surface is energetically favorable, indeed. Thus, we consider the (001) surface of ABO_3 to be TiO_2 terminated in the following.

In polar PTO and BTO, the displacements of the Ti and O atoms occur along the z axis so that **P** is considered to be directed along the [001] direction as well. First, we must formally set up the direction of electric dipole in the unrelaxed supercell assuming, for instance, that O is always above the corresponding cations in each layer along [001], as given in Table I. Then, we can model the two distinct situations alternatively placing the bulklike 3 unit cell thick substrate and relaxed layers against each other along the z axis. In the first case, which we denote as $P_\downarrow$, the direction of P is antiparallel to the surface normal. The second model labeled by $P_\uparrow$ corresponds to the case where all cations are above O before relaxation and, therefore, P is parallel to [001]. In the tetragonal FE structure, both configurations may coexist in the random state as $P_\downarrow$ and $P_\uparrow$ domains separated by a domain wall of <2 nm. To quantify the process of relaxation, we use the cation-anion displacements $\delta=z_O-z_{cation}$ calculated for each AO and TiO layer near the interface. In the bulklike substrate of polar PTO and BTO, the model $P_\uparrow$ means that $\delta<0$ and, vice versa, the case of $P_\downarrow$ models the situation where $\delta>0$.

Figure 1 shows several top monolayers (MLs) of PTO(001) after relaxation. The case $P_\uparrow$ ($P_\downarrow$) is shown on the left (right) side of Fig. 1. The arrows indicate the direction of the dipoles in each ML, while the numbers at the arrows give the intralayer displacements δ in angstroms, calculated between the O and metal atoms along [001]. In state $P_\downarrow$, all

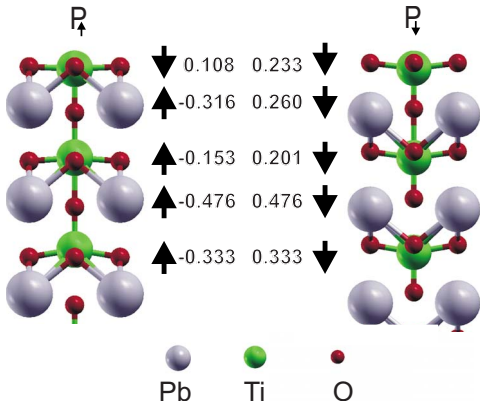

FIG. 1. (Color online) The relaxed top layers of the PTO(001) surface, with polarizations $P_\uparrow$ (left) and $P_\downarrow$ (right). The arrows indicate the direction of the dipole within each layer, while the numbers show the displacements δ in Å between O and Ti/Pb along [001]. For the case of $P_\uparrow$, the sign of δ in the topmost TiO layer is reversed.

dipoles possess the same orientation, which means that O is always above the cation within each layer. In bulk PTO, the intralayer displacement δ is 0.333 Å for the TiO layer and 0.476 Å for the PbO layer. For the three top MLs near the interface, their δ are reduced by 30%–45% with respect to the corresponding bulk values. In the topmost TiO layer, the reduction of δ is ~30%. For the second (PbO) and third (TiO) layers from the interface, we find that their δ is reduced by 45% and 40%, respectively. In the case of $P_\uparrow$, shown in the left panel of Fig. 1, the result of relaxation is rather different. In the third ML, the separation between Ti and O along [001] is 0.153 Å, which is reduced by 54% against the corresponding bulk value. For the second ML, we obtain the reduction of 33%. However, the most significant changes occur in the topmost TiO layer, whose δ is largely reduced by 68%, whereas the dipole is reversed compared to all others. Thus, using the $P_\uparrow$ model and placing all O below the cations, we obtained in the topmost layer the relaxed configuration where O is above Ti. This is similar to the case of $P_\downarrow$.

To investigate the effect of the surface rumpling in perovskites, we repeat the calculations for STO(001) and BTO(001). In Table II, the corresponding results of our zero temperature calculation are listed. For paraelectric STO, we obtain that its TiO-terminated (001) surface after relaxation becomes marginally polar, with a positive rumpling normal to the surface in the top three MLs, where the O atoms are above the cations by <0.12 Å. This is in good agreement with the most recent experimental studies.[26] The positive rumpling predicted for bare surfaces of perovskites leads to a relatively low catalytic activity. With increasing temperature, the rumpling is distorted and it may stimulate further potential catalysis. For the TiO-terminated BTO surface, we have found the details of relaxation similar to those of PTO. In fact, all our results are in good agreement with those reported by Eglitis and Vanderbilt.[12] In the case of $P_\uparrow$, the topmost BTO rumpling of ~0.1 Å, being larger than the corresponding bulk value, is similar to that of highly polar PTO. The sign of δ in the topmost ML of BTO is reversed with respect

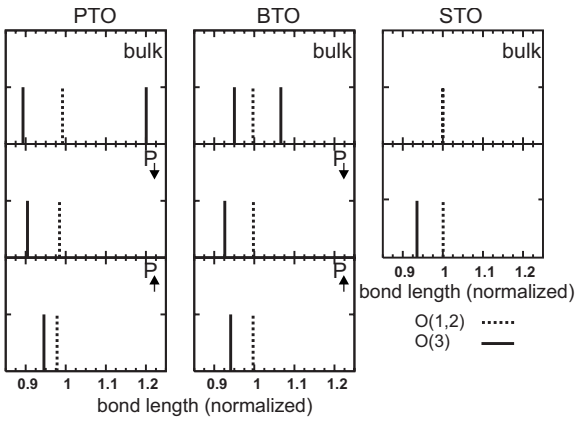

FIG. 2. Ti-O bond lengths in the fivefold coordinated polyhedra of the topmost layer of PTO(001), BTO(001), and STO(001) compared to those obtained in the corresponding bulk structures, with the sixfold coordinated environments.

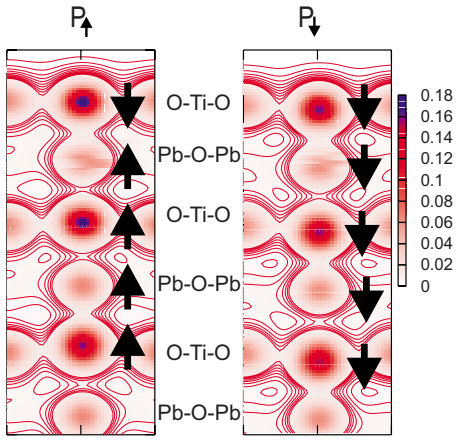

FIG. 3. (Color online) The charge density calculated for the top six layers of $PbTiO_3$(001) and projected on the x-z plane. The two opposite polarization states are shown: $P_\uparrow$ (left) and $P_\downarrow$ (right) where the dipole directions within each layer are labeled by the arrows. In the case of $P_\uparrow$, the isocharge lines of the third TiO layer from the interface show a blockade of the charge transfer along [001].

to all others calculated for the layers situated far down from the interface. In the third ML, δ is 0. The $P_\downarrow$ model yields for BTO(001) the reversal dipole in the second ML, with marginal δ. Thus, we find for the three systems and different arrangements of **P** that the TiO-terminated (001) surfaces prefer the configuration where O is above Ti. In the cubic ABO_3 perovskite structure, each Ti^{4+} ion sits in the regular sixfold coordinated site with all of the Ti-O bonds of equal length, as shown in Fig. 2 for bulk STO.

In the tetragonal perovskite structure, such as t-PTO, the relaxed cluster of O atoms about the sixfold coordinated Ti forms a distorted octahedron, where one of the two bond lengths along [001] is rather short, while another Ti-O bond in the vertical direction is significantly longer than the four other bonds stretching in the equatorial plane. If we exclude the longest Ti-O bond from the consideration using the electrostatic arguments, then the environment for each Ti becomes the fivefold coordinated polyhedra, which is similar to that of Ti at the interface. The left three panels of Fig. 2 compare the Ti-O bond lengths in bulk PTO, normalized to the value of the ideal octahedron in the cubic structure, to those in the polyhedron around fivefold coordinated Ti in the topmost layer. Using the $P_\downarrow$ model for the PTO(001) surface, we obtain the Ti-O bonds whose lengths are similar to those of t-PTO and, hence, nothing dramatic happens in the environment of the topmost Ti. In the case of $P_\uparrow$, the bond length distribution around the topmost Ti is restricted so that the equatorial and vertical bond lengths tend to be equal to each other. Moreover, the closest O atom to the surface Ti is attached along [001] from the opposite side compared to all Ti placed below the surface in the regular crystal structure within $P_\uparrow$. It is clear that the O-Ti-O bond angles for the equatorial Ti-O bonds of the topmost ML must be dramatically changed to compensate the charge distribution around Ti. It appears that these bond angles become $>90°$, as shown in Fig. 1. Therefore, whatever the state of **P** modeled in t-PTO is, the O atoms must relax above Ti on the Ti-O-terminated (001) surface. Regarding BTO, the same conclusions may be drawn.

Figure 3 shows the view of the charge density along [010] calculated for the top six MLs of PTO and projected on the x-z plane of the supercell. The isocharge lines plotted in Fig. 3 for both cases of **P** illustrate the charge transfer across the cell, while the arrows indicate the dipole directions within each ML. In the case of $P_\downarrow$, which is shown in the right panel of Fig. 3, there are three bridges seen between Ti and nearest O. The shortest bond with O, which is always below Ti along [001], has the large population value. In the $P_\uparrow$ state, the charge transfer picture is similar to that of $P_\downarrow$ for the topmost Ti only. Far below the interface (starting from the fifth ML), all Ti have the most populated bond with O which is above Ti. In the third ML, however, the Ti ion is strongly bonded to equatorial oxygens, showing some sort of blockade for the charge transfer along the [001] direction. This may reveal the key electronic state factors behind the surface relaxation of polar FE.

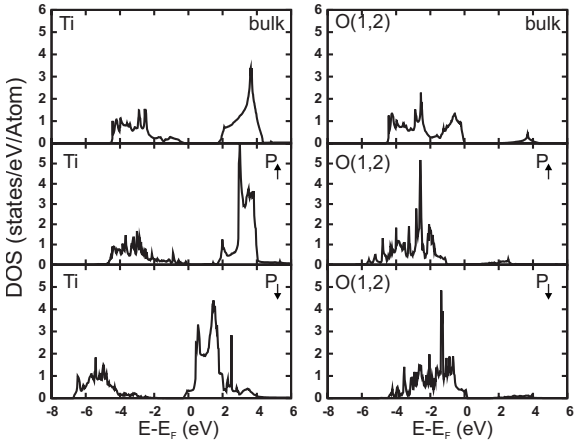

FIG. 4. The Ti- and O_1-resolved DOSs of t-BTO are plotted in the two upper panels where the top of the valence band is taken as zero energy. In the lower panels, the corresponding local DOS of the TiO-terminated (001) surface are plotted for the $P_\uparrow$ and $P_\downarrow$ states.

Recently, Urakami *et al.*[27] have observed the surface conductance of $BaTiO_3$ single crystals in ultrahigh vacuum below T_C. It has been shown that the in-plane conductance is the result of an intrinsic surface electron-hole layer that is due to the surface polarity and not due to O vacancies or some other defects. The *I-V* characteristics show a pronounced difference of conduction between the poled states in BTO. We can explain this difference in a simple way using our *ab initio* results. To reveal the differences between $P_\downarrow$ and $P_\uparrow$, we plot in Fig. 4 the Mulliken site-projected density of states (DOS) of the BTO(001) surface for both cases of polarization. The Ti and O DOSs for the topmost ML are shown in comparison with the corresponding DOS of *t*-BTO. For bulk BTO, Fig. 4 shows a pronounced insulating band gap of 2 eV. The value is typically underestimated by the LDA approximation of DFT. Comparing the Ti and O DOSs of *t*-BTO and the topmost ML of BTO(001), we see a spectacular change of the electronic states occurring due to the surface relaxation and variation of **P**. The major DOS features can be summarized as follows. In the case of $P_\uparrow$, a few O states appear in the band gap, while the Ti DOS is not affected. For the $P_\downarrow$ poled state, the Ti lower conduction band, being shifted downward in energy by $\sim$2 eV, significantly contributes to the DOS in the band gap region. This causes the metallic behavior of the topmost ML in the case of $P_\downarrow$, yielding a rather large in-plane conductance. In the case of $P_\uparrow$, the Ti states have a gap at E_f, which is related to a tiny in-plane conductance. Depending on the polarization direction the topmost ML undergoes, a transition from metallic to oxide behavior shows metallic or oxide behavior. As a consequence, the in-plane conductance changes drastically, which is a reasonable explanation of the experimental results by Urakami *et al.*[27]

In summary, from the *ab initio* basis of our work, we have shown that the intrinsic ferroelectricity in polar perovskites is suppressed by $\sim$30% in the surface region. For both cases of polarization direction, the TiO-terminated surface of BTO and PTO forms an electric dipole where the O atoms are shifted $>$0.1 Å above Ti. Nevertheless, the electronic structure of the surface layer changes from metallic to oxide behavior under the reversal of polarization, which changes the surface conductance drastically.[27] This may have important implications in the design of multiferroic nanodevices.

[1] M. Dawber, K. M. Rabe, and J. F. Scott, Rev. Mod. Phys. **77**, 1083 (2005).
[2] H. Zheng, J. Wang, S. E. Lofland, L. M.-A. Z. Ma, T. Zhao, L. Salamanca-Riba, S. R. Shinde, S. B. Ogale, F. Bai, and D. Viehland, Science **303**, 661 (2004).
[3] W. Eerenstein, N. D. Mathur, and J. F. Scott, Nature (London) **442**, 759 (2006).
[4] J. Padilla and D. Vanderbilt, Phys. Rev. B **56**, 1625 (1997).
[5] R. E. Cohen, Ferroelectrics **194**, 323 (1997).
[6] G. Sághi-Szabó, R. E. Cohen, and H. Krakauer, Phys. Rev. Lett. **80**, 4321 (1998).
[7] E. Heifets, R. I. Eglitis, E. A. Kotomin, J. Maier, and G. Borstel, Phys. Rev. B **64**, 235417 (2001).
[8] J. B. Neaton and K. M. Rabe, Appl. Phys. Lett. **82**, 1586 (2003).
[9] Y. Umeno, T. Shimada, T. Kitamura, and C. Elsässer, Phys. Rev. B **74**, 174111 (2006).
[10] Y. X. Wang, M. Arai, T. Sasaki, and C. L. Wang, Appl. Phys. Lett. **88**, 091909 (2006).
[11] S. Lisenkov and L. Bellaiche, Phys. Rev. B **76**, 020102(R) (2007).
[12] R. I. Eglitis and D. Vanderbilt, Phys. Rev. B **76**, 155439 (2007).
[13] J. Junquera and P. Ghosez, Nature (London) **422**, 506 (2003).
[14] N. A. Spaldin, Science **304**, 1606 (2004).
[15] D. D. Fong, G. B. Stephenson, S. K. Streiffer, J. A. Eastman, O. Auciello, P. H. Fuoss, and C. Thompson, Science **304**, 1650 (2004).
[16] G. Kresse and J. Furthmüller, Phys. Rev. B **54**, 11169 (1996).
[17] P. Ghosez and J. Junquera, *Handbook of Theoretical and Computational Nanotechnology*, edited by M. Rieth and W. Schommers (American Scientific Publisher, Stevenson Ranch, CA, USA, 2006), Vol. 7, Chap. 134.
[18] H. Mestric, R.-A. Eichel, T. Kloss, K.-P. Dinse, So. Laubach, St. Laubach, P. C. Schmidt, K. A. Schonau, M. Knapp, and H. Ehrenberg, Phys. Rev. B **71**, 134109 (2005).
[19] T. Toshio, K.-H. Hellwege, H. Landolt, R. Börnstein, and O. Madelung, in *Ferro- and Antiferroelectric Substances*, edited by K.-H. Hellwege and A. M. Hellwege, Landolt-Börnstein, Group III, Vol. 3 (Springer-Verlag, Berlin, 1981).
[20] V. Gavrilyachenko, R. Spinko, M. Martynenko, and E. Fesenko, Sov. Phys. Solid State **12**, 1532 (1970).
[21] H. H. Wieder, Phys. Rev. **99**, 1161 (1955).
[22] R. D. King-Smith and D. Vanderbilt, Phys. Rev. B **47**, 1651 (1993).
[23] R. Resta, Rev. Mod. Phys. **66**, 899 (1994).
[24] R. D. King-Smith and D. Vanderbilt, Phys. Rev. B **49**, 5828 (1994).
[25] H. J. Monkhorst and J. D. Pack, Phys. Rev. B **13**, 5188 (1976).
[26] P. A. W. van der Heide, Q. D. Jiang, Y. S. Kim, and J. W. Rabalais, Surf. Sci. **473**, 59 (2001).
[27] Y. Urakami, M. Yamato, and Y. Watanabe, Ferroelectrics **346**, 32 (2007).